

Supporting information for:

β -deprotonation in the mechanism of formate oxidation by

$[\text{Ni}(\text{P}^{\text{R}}_2\text{N}^{\text{R}'}_2)_2(\text{CH}_3\text{CN})](\text{BF}_4)_2$ complexes

Candace S. Seu[†], Aaron M. Appel[‡], Michael D. Doud[†], Daniel L. DuBois[‡], and Clifford P. Kubiak^{†}*

[†]*Department of Chemistry & Biochemistry, University of California, San Diego, 92093 and*

[‡]*Chemical and Materials Sciences Division, Pacific Northwest National Laboratory, Richland, WA 99352*

| Table of Contents | Page |
|--|-------------|
| Synthetic procedure for $\text{P}^{\text{Cy}}_2\text{N}^{\text{PhCF}_3}_2$ | 2 |
| Synthetic procedure for $[\text{Ni}(\text{P}^{\text{Cy}}_2\text{N}^{\text{PhCF}_3}_2)_2(\text{CH}_3\text{CN})](\text{BF}_4)_2$ | 2 |
| Crystallographic details of $\text{Ni}(\text{P}^{\text{Cy}}_2\text{N}^{\text{PhOMe}}_2)_2(\text{CH}_3\text{CN})](\text{BF}_4)_2$ | 3 |
| Figure S1-2. Crystal structures of $\text{Ni}(\text{P}^{\text{Cy}}_2\text{N}^{\text{PhOMe}}_2)_2(\text{CH}_3\text{CN})](\text{BF}_4)_2$ | 3 |
| Table S1. Selected bond lengths and angles for $\text{Ni}(\text{P}^{\text{Cy}}_2\text{N}^{\text{PhOMe}}_2)_2(\text{CH}_3\text{CN})](\text{BF}_4)_2$ | 4 |
| Figure S3. Eyring plot | 5 |
| Figure S4. Arrhenius plot | 5 |

Synthetic procedures

Synthesis of $\text{P}^{\text{Cy}}_2\text{N}^{\text{PhCF}_3}_2$. Cyclohexylphosphine (0.53 mL, 4.0 mmol) was placed in a Schlenk flask and cannula transferred into a flask containing paraformaldehyde (0.24 g, 8.0 mmol) in 1-butanol 12 (mL). The reaction was stirred under reflux for 2 h and the white suspension became clear. 4-trifluoromethylaniline (0.50 mL, 4.0 mmol) was added via syringe and the reaction was further refluxed for 3 h, then cooled. A white precipitate began forming within 30 minutes of the 2nd reflux, and after cooling, the solid was collected by cannula filtration, rinsed twice with ethanol, and dried under vacuum to yield 0.85 g (1.4 mmol, 71%) of $\text{P}^{\text{Cy}}_2\text{N}^{\text{PhCF}_3}_2$ ligand. ^1H NMR (CDCl_3 , 300 MHz, CHCl_3) δ_{H} [ppm]: 7.4 (4H, d, $J_{23} = 9$ Hz, Ar 2,6-H), 6.6 (4H, d, $J_{32} = 9$ Hz, Ar 3,5-H), 4.4-3.7 (8H, m, PCH_2N), 2.0-1.3 (22H, m, Cy). $^{31}\text{P}\{^1\text{H}\}$ NMR (CDCl_3 , 121 MHz, H_3PO_4) δ_{P} [ppm]: -36.1 (s, major), -28.2 (s, minor), 10:1 intensities. Elemental analysis calculated for $\text{C}_{30}\text{H}_{38}\text{F}_6\text{P}_2\text{N}_2$: C, 59.8; H, 6.4; N, 4.65. Found: C, 59.6; H, 6.3; N, 4.5.

Synthesis of $[\text{Ni}(\text{P}^{\text{Cy}}_2\text{N}^{\text{PhCF}_3}_2)_2(\text{CH}_3\text{CN})](\text{BF}_4)_2$. $\text{P}^{\text{Cy}}_2\text{N}^{\text{PhCF}_3}_2$ (360 mg, 0.60 mmol) was added to a blue solution of $[\text{Ni}(\text{CH}_3\text{CN})_6](\text{BF}_4)_2$ (140 g, 0.30 mmol) in acetonitrile (12 mL). The initially cloudy red suspension was stirred at room temperature overnight until the ligand dissolved. The dark red solution was cannula filtered to remove unreacted ligand and dried under vacuum. The metal-ligand complex is rather unstable and tends to dissociate to mono-ligand complexes at room temperature in the presence of non-polar solvents and high concentrations of anions. This dissociation is signaled by a color change to yellow, corresponding to formation of square-planar Ni(II) complexes. Yield = 250 mg (0.17 mmol, 56%). Attempts to purify the complex by crystallization and to obtain crystals via liquid and vapor diffusion of diethyl ether into a concentrated acetonitrile solution of the red homoleptic Ni(II) complex at various temperatures yielded highly disordered crystals of the above-mentioned square-planar complexes. ^1H NMR (CDCl_3 , 300 MHz, CHCl_3) [ppm]: δ_{H} 7.8-7.6 (2H, d, $J_{23} = 8.7$ Hz, $J_{25} = 39$ Hz, Ar 2,6-H), 6.6 (4H, d, $J_{32} = 9$ Hz, Ar 3,5-H), 4.4-3.7 (8H, m, PCH_2N), 2.0-1.3 (22H, m, Cy). $^{31}\text{P}\{^1\text{H}\}$ NMR (CDCl_3 , 121 MHz, H_3PO_4) [ppm]: δ_{P} 7.28 (s).

Crystallographic details of $\text{Ni}(\text{P}^{\text{Cy}}_2\text{N}^{\text{PhOMe}}_2)_2(\text{CH}_3\text{CN})](\text{BF}_4)_2$

Crystals of $\text{Ni}(\text{P}^{\text{Cy}}_2\text{N}^{\text{PhOMe}}_2)_2(\text{CH}_3\text{CN})](\text{BF}_4)_2$ were found to have crystallized on space group $C2/c$ such that the Ni-acetonitrile vector was located on the C_2 axis of symmetry. As a result, the phenyl and cyclohexyl substituents off N and P, respectively, appeared disordered due to slight conformational variations between the two halves of the molecule. These rings were modeled simultaneously by setting analogous atoms in different conformations to partial occupancy. It should be noted that this disorder is the root cause of several false checkCIF alerts regarding short intramolecular H-H contacts and missing hydrogen bond acceptors. Despite these alerts and extensive disorder, the crystal data was modeled satisfactorily to 4.19% (using 2θ). Attempts to model the structure in a space group of lower symmetry did not converge.

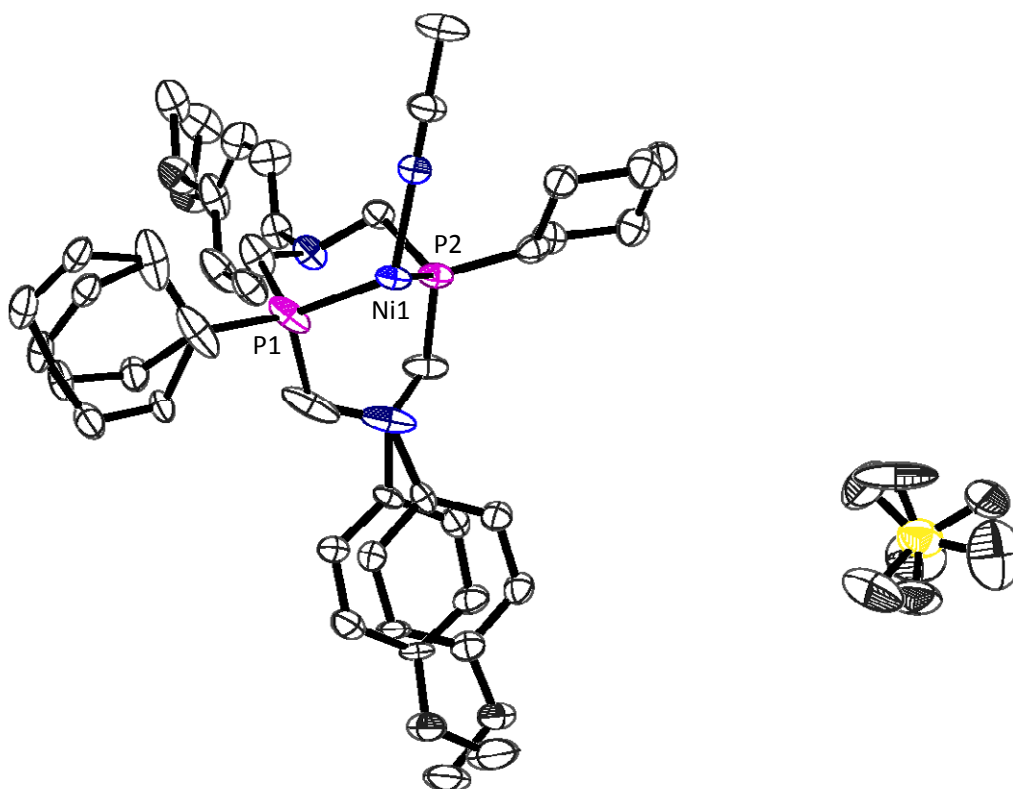


Figure S1. Thermal ellipsoid plot of $\text{Ni}(\text{P}^{\text{Cy}}_2\text{N}^{\text{PhOMe}}_2)_2(\text{CH}_3\text{CN})](\text{BF}_4)_2$ asymmetric unit, showing ligand disorder (note that only half of the complex is contained in each asymmetric unit). Hydrogen atoms have been omitted for clarity.

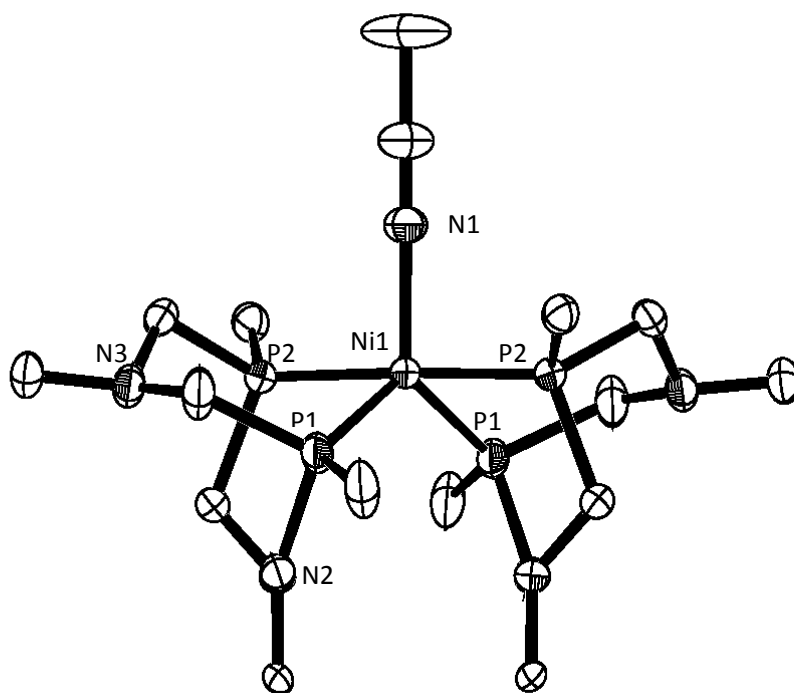
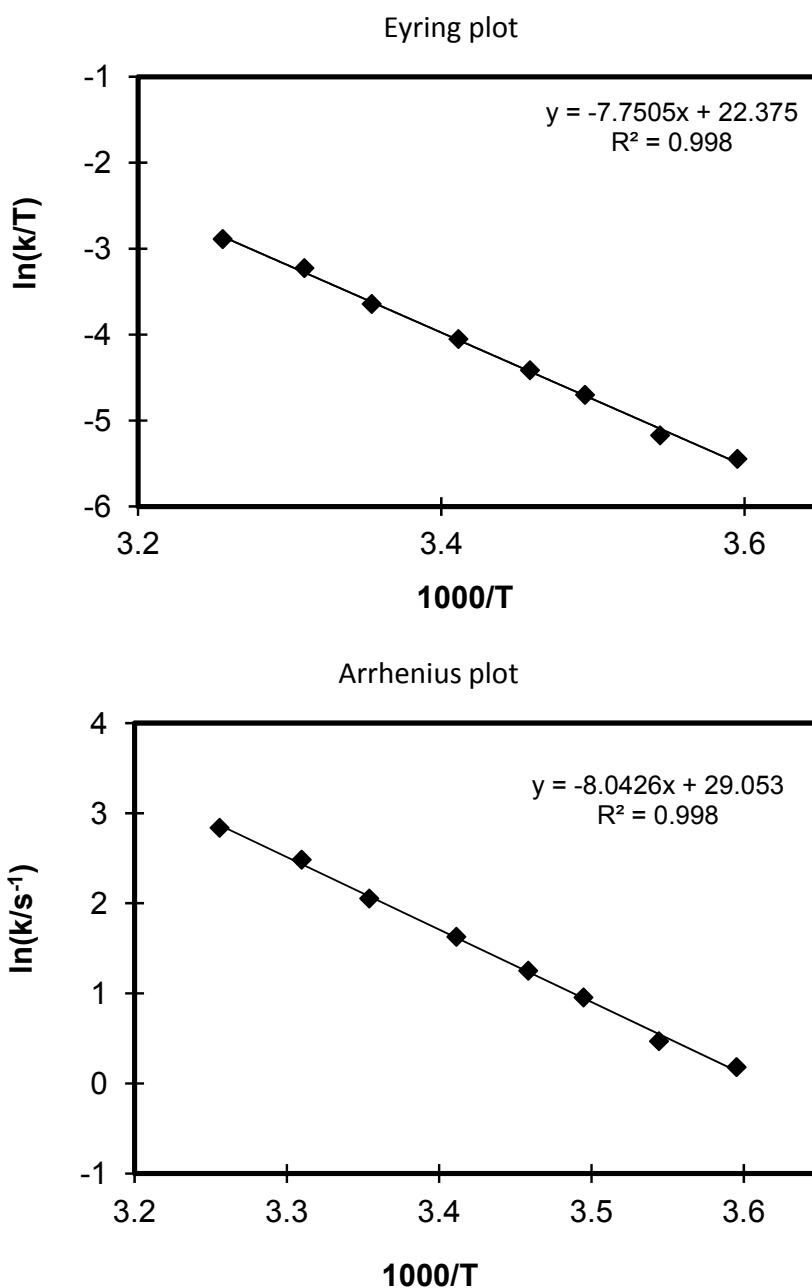


Figure S2. Thermal ellipsoid plot of $\text{Ni}(\text{P}^{\text{Cy}}_2\text{N}^{\text{PhOMe}}_2)_2(\text{CH}_3\text{CN})](\text{BF}_4)_2$ showing ligand conformation around Ni core. Hydrogen atoms and counter ions have been omitted for clarity.

Table S1. Selected bond lengths and angles for $\text{Ni}(\text{P}^{\text{Cy}}_2\text{N}^{\text{PhOMe}}_2)_2(\text{CH}_3\text{CN})](\text{BF}_4)_2$.

| | Distance (Å) | | Angle (°) |
|------------|--------------|------------------|-----------|
| Ni(1)-N(1) | 1.993(3) | P(2)-Ni(1)-P(1) | 81.89 |
| Ni(1)-P(1) | 2.2332(6) | P(2)-Ni(1)-P(1b) | 97.14 |
| Ni(1)-P(2) | 2.2293(6) | P(1)-Ni(1)-P(1b) | 119.91 |
| | | P(2)-Ni(1)-P(2b) | 178.08 |
| Ni(1)⋯N(2) | 3.318 | | |
| Ni(1)⋯N(3) | 3.847 | N(1)-Ni(1)-P(1) | 120.04 |
| | | N(1)-Ni(1)-P(2) | 90.96 |

Figure S3 and S4. Eyring and Arrhenius plots for formate oxidation by $[\text{Ni}(\text{P}^{\text{Ph}}_2\text{N}^{\text{PhOMe}}_2)_2]^{2+}$, calculated from temperature-dependent TOFs.



Acknowledgments

C.S.S., M.D.D., and C.P.K. gratefully acknowledge the Joint Center for Artificial Photosynthesis, a DOE Energy Innovation Hub that is supported through the Office of Science of the U.S. Department of Energy for funding the mechanistic studies, and a grant from the Air Force Office of Scientific Research

through the MURI program (AFOSR Award No. FA9550-10-1-0572) for funding synthetic studies. C.S.S. acknowledges support from the National Science Foundation via a Graduate Research Fellowship (Grant No. DGE0707423) as well as via (CHE-0741968). A.M.A. and D.L.D. were supported by the U.S. Department of Energy, Office of Science, Office of Basic Energy Sciences, Division of Chemical Sciences, Biosciences and Geosciences. Pacific Northwest National Laboratory (PNNL) is a multiprogram national laboratory operated for DOE by Battelle. C.S.S. wishes to thank A.R. Rheingold, B.R. Galan, S.D. Glover, K.A. Grice, B. Kumar, and E.E. Benson for helpful discussions on electrochemistry and crystallography.